Catalysis Letters 20 (1993) 191–201

Dehydrogenation of ethylbenzene over TiO_2–Fe_2O_3 and ZrO_2–Fe_2O_3 mixed oxide catalysts

Jung-Chung Wu [1]

Refining and Manufacturing Research Center, Chinese Petroleum Corporation,
239 Min-Sheng S. Road, Chia-Yi, Taiwan 60036, ROC

Der-Sun Liu and An-Nan Ko

Department of Chemistry, Tunghai University, Taichung, Taiwan, ROC

Received 11 December 1992; accepted 1 May 1993

The mixed metal oxides TiO_2–Fe_2O_3 and ZrO_2–Fe_2O_3 were examined as potential catalysts for the dehydrogenation reaction of ethylbenzene. The acidic and basic properties and surface area, pore volume and pore size distribution of these catalysts were measured. The catalytic activities can be correlated very well with the surface area and the acidity and basicity of ZrO_2–Fe_2O_3 catalysts. However, for TiO_2–Fe_2O_3 catalysts, the surface area, the amount of acidic and basic sites and $TiFe_2O_5$ crystallinity are all important factors affecting the catalytic activities for ethylbenzene dehydrogenation. A synergistic effect was found for the TiO_2–Fe_2O_3 and ZrO_2–Fe_2O_3 catalyst system and also for the TiO_2–Fe_2O_3–ZrO_2 system, i.e. the activities of these catalysts can be ranked in the following order: TiO_2–Fe_2O_3–$ZrO_2 > TiO_2$–$Fe_2O_3 > ZrO_2 > Fe_2O_3 > TiO_2$. Meanwhile, all of these catalysts showed higher activities than the conventional potassium-promoted iron catalysts.

Keywords: Dehydrogenation of ethylbenzene; TiO_2–Fe_2O_3; ZrO_2–Fe_2O_3; TiO_2–Fe_2O_3–ZrO_2 mixed oxides; bifunctional mechanism; synergistic effect; styrene

1. Introduction

The catalytic dehydrogenation of ethylbenzene is of industrial importance in the manufacturing of styrene. Iron oxide promoted with alkali is used mostly as the catalyst in the industrial process for this reaction [1–3]. In our previous papers [4–7] the relationship between the surface property and the activity of ethylbenzene dehydrogenation over TiO_2–ZrO_2 and the binary oxides combining TiO_2 with other first period transition metal oxides was extensively studied. An acid–base bifunctional mechanism was proposed for ethylbenzene dehydrogenation over

---

[1] To whom correspondence should be addressed.

these binary oxides. This bifunctional mechanism was also found in the selective oxidation or oxidative dehydrogenation reaction over Al_2O_3 [8], SnO_2–P_2O_5 [9,10], Fe_2O_3-based mixed oxides [11–13], and Na–SiO_2·Al_2O_3 [14,15] catalysts. The catalytic activities of various kinds of reactions over TiO_2-based catalysts have been reviewed by Matsuda and Kato [16].

The relations between catalytic activity and acidic and basic properties of TiO_2 [17], ZrO_2 [18], and mixed oxides such as TiO_2–SiO_2 [17–21], TiO_2–MgO [22], TiO_2–V_2O_5 [23], TiO_2–MoO_3, TiO_2–Al_2O_3 [24], TiO_2–ZnO [25], TiO_2–SnO_2, TiO_2–SnO [26], TiO_2–NiO [27], and TiO_2–ZrO_2 [4–7,28] etc. have been previously investigated.

In this work, the acid–base properties of a series of TiO_2–Fe_2O_3 and ZrO_2–Fe_2O_3 catalysts with different molar ratios of TiO_2 to Fe_2O_3 and ZrO_2 to Fe_2O_3 were measured and the catalytic activities of ethylbenzene dehydrogenation were examined. The results in this work showed a synergistic effect for the mixed binary oxides TiO_2–Fe_2O_3 and ZrO_2–Fe_2O_3.

2. Experimental

2.1. PREPARATION OF CATALYSTS

TiO_2–Fe_2O_3 catalysts with different molar ratios of TiO_2 to Fe_2O_3 were prepared by coprecipitation of a mixed solution of titanium tetrachloride and ferric chloride in anhydrous alcohol with aqueous ammonia (28%). The precipitate was aged over water bath for 2 h and washed with deionized water until no chloride ions were detected with Ag^+ in the filtrate, then dried at 110°C for 4 h, followed by calcination at 700°C in air for 2 h. The ZrO_2–Fe_2O_3 catalysts with different molar ratios of ZrO_2 to Fe_2O_3 were also prepared by the same procedure with zirconium tetrachloride and ferric chloride compounds.

2.2. ACIDITY AND BASICITY MEASUREMENT

The acidity and basicity of the catalysts were measured by *n*-butylamine and acetic acid adsorption, respectively, as described in our previous papers [4–7]. The catalyst was first put in a desiccator with saturated *n*-butylamine or acetic acid vapor at room temperature for 48 h. Then, the weight loss of the adsorbed sample was measured by a TG apparatus at programmed temperature 20°C/min ($40 \rightarrow 500$°C).

2.3. SURFACE AREA, PORE SIZE, PORE VOLUME AND X-RAY ANALYSIS

The specific surface areas of catalysts were determined by applying the BET method. Crystallinity of the catalysts was characterized by X-ray powder diffraction pattern over the range of $2\theta = 4$–$60°$ with Mn filtered Fe K_α radiation. The pore volume and average pore size of the catalysts were measured with a mercury porosimeter.

2.4. REACTION EQUIPMENT AND EXPERIMENTAL PROCEDURE

The catalytic reaction was carried out in a continuous flow fixed-bed reactor. The reactor was a quartz glass tube with an inside diameter of 1.6 cm, which was packed from top to bottom with layers of inert ceramic, catalyst particles (0.8 g, 30–60 mesh) and inert ceramic. The catalyst bed was first heated up to 600°C with air at a flow rate of 360 ml/min for 2 h and then purged with nitrogen stream for 30 min. Then the reaction was studied under the following conditions: reaction temperature, 570°C; total pressure, 760 mmHg; WHSV = 11.3.

3. Results and discussion

The reactions of ethylbenzene (EB) dehydrogenation over TiO_2–Fe_2O_3 and ZrO_2–Fe_2O_3 catalysts give styrene (ST) as the major product and small amounts of benzene and toluene as by-products. In this study, catalyst performances will be expressed according to the following formulas:

$$\text{ethylbenzene conversion: } C\ (\%) = \frac{EB_{\text{inlet}} - EB_{\text{outlet}}}{EB_{\text{inlet}}} \times 100\,,$$

$$\text{product selectivity: } S_i\ (\%,\text{mol}) = \frac{\text{product}(i)}{EB_{\text{inlet}} - EB_{\text{outlet}}} \times 100\,,$$

$$\text{product yield: } Y_i\ (\%,\text{mol}) = \frac{\text{product}(i)}{EB_{\text{inlet}}} \times 100 = C \times S_i\,.$$

3.1. EFFECT OF CATALYST COMPOSITION

The relation between ethylbenzene conversion and the composition of TiO_2–Fe_2O_3 is shown in fig. 1, where we refer to the ethylbenzene conversion as the activity index and all the catalysts were calcined at 700°C for 2 h. By itself, TiO_2 or Fe_2O_3 are impractical as a catalyst for the dehydrogenation of ethylbenzene. For example, the conversions of this reaction are 28 and 20% for K and TiO_2, respectively. However, the binary oxide TiO_2–Fe_2O_3 is very effective. The activity increased with the increase of TiO_2 content in TiO_2–Fe_2O_3 through a maximum at 70 mol% of TiO_2 and then decreased drastically as shown in fig. 1. The amounts of both acidic and basic sites of TiO_2–Fe_2O_3 with different compositions were measured by the adsorption of basic and acidic molecules in the vapor phase. The results are shown in fig. 2. It indicates that both acidity and basicity increased by

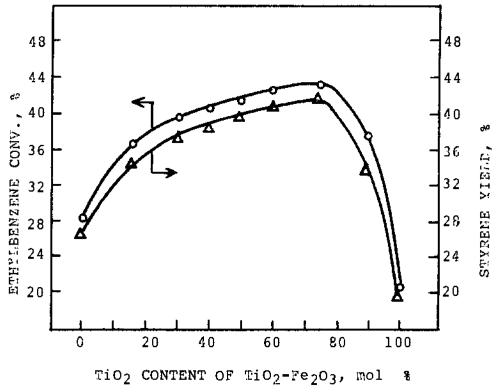

Fig. 1. Effect of catalyst composition on the conversion of ethylbenzene and the yield of styrene over TiO_2–Fe_2O_3 catalysts; reaction temperature, 570°C; WHSV = 11.3.

the mixing of TiO_2 and Fe_2O_3 up to the catalysts with 40–50 mol% of TiO_2. The relationship between the surface area and composition of TiO_2–Fe_2O_3 is also shown in fig. 2, where the surface areas increased by the mixing of TiO_2 and Fe_2O_3 and attained a maximum at about 40–50 mol% of TiO_2. Table 1 shows the relative acidity, basicity and relative turnover frequency (RTOF) of TiO_2–Fe_2O_3 mixed oxide catalysts with various TiO_2 contents, where the relative acidity and basicity are defined as the amount of *n*-butylamine and acetic acid adsorbed in mmol per unit surface area. The relative turnover frequency is defined as the mol conversion of ethylbenzene per unit surface area under the same reaction conditions. It indicates that the relative TOF of pure Fe_2O_3 and TiO_2 are higher than those of mixed metal oxides. The relative TOF can be correlated with the relative acidity and basicity. The catalyst with 50 mol% of TiO_2 gave the highest surface area and, therefore, the highest acid and base amount.

In a previous paper we have proposed an acid–base bifunctional mechanism for the dehydrogenation of ethylbenzene over TiO_2–ZrO_2 catalysts [4]. The catalytic

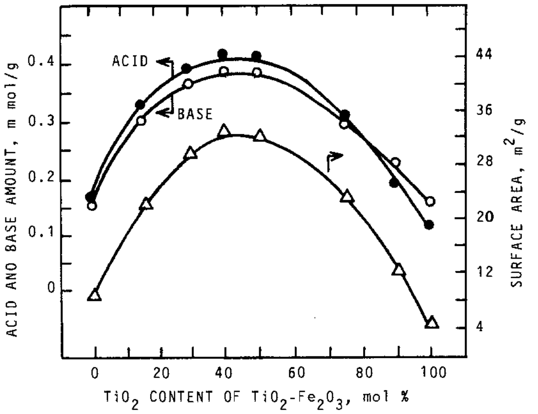

Fig. 2. The acid and base amount and surface area of TiO_2–Fe_2O_3 catalysts with various compositions; calcination temperature, 700°C.

Table 1
The physical properties and catalytic activities of TiO_2–Fe_2O_3 catalysts with various compositions

	mol% of TiO_2								Shell 105
	0	15	30	40	50	75	90	100	
acid amount (mmol/g)	0.17	0.33	0.39	0.41	0.41	0.31	0.20	0.12	0.08
base amount (mmol/g)	0.15	0.31	0.37	0.38	0.38	0.30	0.22	0.15	7.82
surface area (m^2/g)	10	22	30	32	32	23	12	4	28
pore vol. (c.c/g)	0.16	0.20	0.21	0.24	0.24	0.23	0.09	0.04	–
av. pore diam. (Å)	280	150	120	110	105	105	100	50	–
relative acidity ($mmol/m^2$)	0.017	0.015	0.013	0.013	0.013	0.013	0.017	0.030	0.003
relative basicity ($mmol/m^2$)	0.015	0.014	0.012	0.012	0.012	0.013	0.018	0.038	0.279
relative TOF (mol% conv./m^2)	2.80	1.64	1.27	1.28	1.31	1.87	3.08	5.00	1.07
conv. (mol%)	28	36	38	41	42	43	37	20	30

activities can be correlated well with the acid–base properties (especially the basicity) of the catalysts. However, in the present work, the catalytic activities of ethylbenzene dehydrogenation over TiO_2–Fe_2O_3 cannot be correlated very well with the acidity, basicity and surface area. Therefore, there must be another significant factor affecting the catalytic activity.

In order to identify this factor, we studied the crystal structure of TiO_2–Fe_2O_3 catalysts by X-ray powder diffraction. Fig. 3 shows the XRD patterns of TiO_2–Fe_2O_3 with various compositions, where all of the catalysts were calcined at 700°C. The crystallinity of TiO_2 (rutile), Fe_2O_3 (hematite), and $TiFe_2O_5$ were identified by the peaks occurring at 2θ (deg) = 27.4 (vs), 35.9 (s), 41.2 (m), 54.3 (s); 24.2 (m), 33.2 (vs), 35.7 (s), 49.5 (m), 54.1 (m); and 18.0 (m), 25.5 (vs), 32.5 (s), 36.8 (m), 49.0 (m), respectively. We found that (i) $TiFe_2O_5$ crystal formed when the amount of TiO_2 was above 25 mol% and the maximum crystallinity of $TiFe_2O_5$ was obtained at 75 mol% of TiO_2, (ii) rutile of TiO_2 crystallized gradually when the amount of TiO_2 was above 50 mol%, (iii) Fe_2O_3 (hematite) crystallinity decreased with the addition of TiO_2.

From the results of the X-ray diffraction study, we speculate that the highest activity of the catalyst with 75 mol% of TiO_2 may be due to the formation of $TiFe_2O_5$ crystal. The drastic decrease of catalytic activity may be caused by lower acidity, basicity, surface area, and crystallinity of $TiFe_2O_5$. The pore size distribution and

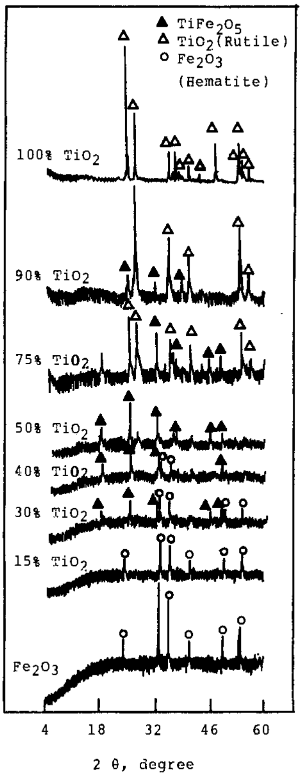

Fig. 3. X-ray diffraction of TiO_2–Fe_2O_3 catalysts with various compositions; calcination temperature, 700°C.

pore volume of the catalysts were also measured. The results are shown in table 1. It indicates that the average pore diameter decreased with the increase of TiO_2 content. However, the pore volume of the catalysts increased through a maximum and then decreased drastically with the increase of TiO_2 content.

From the results of acidity, basicity, and X-ray diffraction study, we proposed that the highest activity of the catalyst with 75 mol% of TiO_2 was due to the formation of $TiFe_2O_5$ crystal. However, the catalyst with 15 mol% of C also showed a good activity, although there is no $TiFe_2O_5$ crystal in the catalyst. Thus, we speculated that both the amount of acidic and basic sites and $TiFe_2O_5$ crystallinity are all important factors affecting the catalytic activity of the dehydrogenation of ethylbenzene over TiO_2–Fe_2O_3 catalysts. This phenomenon was also found in our previous work for the TiO_2–ZrO_2 system [5].

3.2. EFFECT OF CATALYST COMPOSITION FOR THE ZrO_2–Fe_2O_3 SYSTEM

The relation between ethylbenzene conversion and the composition of ZrO_2–Fe_2O_3 is shown in fig. 4, where all of the catalysts were calcined at 700°C for 2 h.

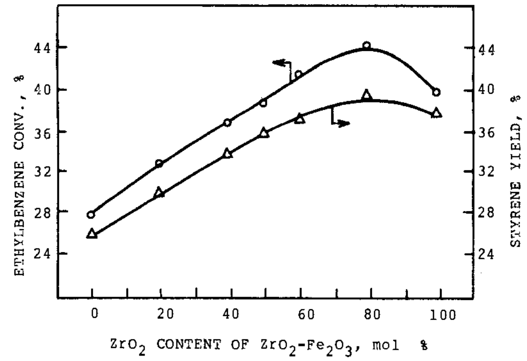

Fig. 4. Effect of catalyst composition on the conversion of ethylbenzene and the yield of styrene over ZrO_2–Fe_2O_3 catalysts; reaction temperature, 570°C; WHSV = 11.3.

The activities of the catalysts increased with the increase of ZrO_2 content in ZrO_2–Fe_2O_3 through a maximum at about 80 mol% of ZrO_2 and then decreased. Most of ZrO_2–Fe_2O_3 catalysts showed a higher activity than the commercial catalyst Shell 105 under the reaction conditions: 570°C and 11.3 WHSV. The amounts of both acidic and basic sites of ZrO_2–Fe_2O_3 with different compositions were measured. The results are shown in fig. 5. It indicates that both acidity and basicity increased with the addition of ZrO_2 to the pure metal oxide Fe_2O_3 through a maximum at 80 mol% of ZrO_2. The relationship between the surface area and composition of ZrO_2–Fe_2O_3 is also shown in fig. 5, where the surface area also increases with the increase of ZrO_2 content and attained a maximum at about 80 mol% of ZrO_2. Table 2 shows the relative turnover frequency of ZrO_2–Fe_2O_3 mixed oxide catalysts with various ZrO_2 contents. It indicates that the relative acidity and basicity of mixed oxides are almost the same. Comparing the results from tables 1 and

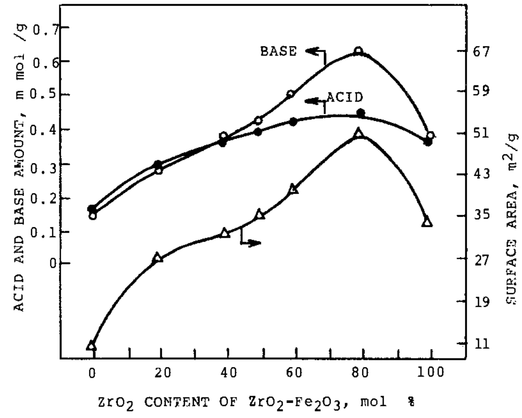

Fig. 5. The acid and base amount and surface area of ZrO_2–Fe_2O_3 catalysts with various compositions; calcination temperature, 700°C.

Table 2
The physical properties and catalytic activities of ZrO_2–Fe_2O_3 catalysts with various compositions

	mol% of ZrO_2							Shell 105
	0	20	40	50	60	80	100	
acid amount (mmol/g)	0.17	0.30	0.35	0.38	0.42	0.43	0.34	0.08
base amount (mmol/g)	0.15	0.27	0.36	0.43	0.50	0.61	0.36	7.82
surface area (m^2/g)	10	28	30	32	37	49	32	28
pore vol. (c.c/g)	0.16	0.26	0.23	0.21	0.24	0.24	0.23	–
av. pore diam. (Å)	280	95 170	145	100	90	70	70	–
relative acidity ($mmol/m^2$)	0.017	0.011	0.012	0.012	0.011	0.009	0.011	0.003
relative basicity ($mmol/m^2$)	0.015	0.010	0.012	0.013	0.013	0.012	0.011	0.279
relative TOF (mol% conv./m^2)	2.80	1.18	1.23	1.22	1.14	0.90	1.25	1.07
conv. (mol%)	28	33	37	39	42	44	40	30

2, we find that the relative turnover frequencies of ethylbenzene dehydrogenation of pure ZrO_2, Fe_2O_3 and TiO_2 are 1.25, 2.80 and 5.00, respectively. However, the conversions over these catalysts are 40, 28 and 20%, respectively, due to the significant difference of surface area. Comparing the results of figs. 4 and 5, we find that the catalytic activities can be correlated very well with the surface area and the acidity and basicity of ZrO_2–Fe_2O_3 catalysts. The pore size distribution and pore volume of the catalysts were also measured. The results are shown in table 2. It indicates that the average pore diameter decreased with the increase of ZrO_2 content.

Fig. 6 shows the XRD patterns of ZrO_2–Fe_2O_3 with various compositions, where all of the catalysts were calcined at 700°C. The crystallinities of ZrO_2 (monoclinic) and ZrO_2 (cubic) were identified by the peaks occurring at 2θ (deg) = 24.1 (m), 28.2 (vs), 31.5 (s), 34.3 (m), 50.2 (m) and 30.5 (vs), 35.4 (m), 50.7 (s), respectively. It indicates that the crystallinity of ZrO_2 (cubic) increases with the increase of ZrO_2 content in the range of 20–80%. It also indicates that the crystal structure of ZrO_2 was changed from pure monoclinic to pure cubic form after the addition of 20% of Fe_2O_3. The ZrO_2–Fe_2O_3 catalyst with this composition happened to show the highest activity. Therefore, it may probably be assumed that ZrO_2 in cubic structure will be beneficial to the activity of the ethylbenzene dehydrogenation reaction.

Fig. 7 shows the effect of reaction temperature on the activity and selectivity of ethylbenzene dehydrogenation over ZrO_2–Fe_2O_3 (80/20) and the commercial cata-

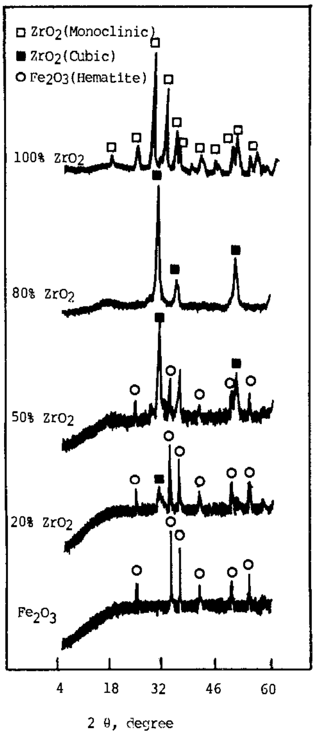

Fig. 6. X-ray diffraction of ZrO_2–Fe_2O_3 catalysts with various compositions; calcination temperature, 700°C.

lyst Shell 105. It indicates that the activity increased and the selectivity decreased with the increase of reaction temperature for both of the catalysts. It also indicates that the decrease of selectivity was slower than the increase of activity for both ZrO_2–Fe_2O_3 (80/20) and the commercial Shell 105 catalyst.

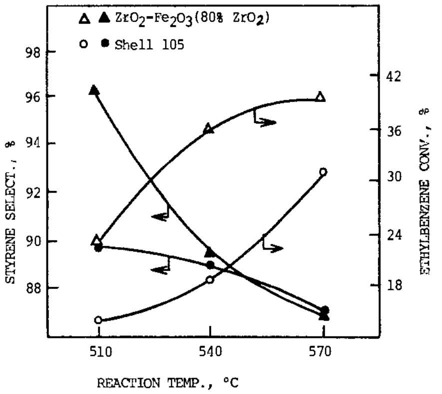

Fig. 7. Effect of reaction temperature on the conversion of ethylbenzene and the selectivity of styrene over ZrO_2–Fe_2O_3 catalyst with 80% ZrO_2 and commercial Shell 105 catalyst.

3.3. SYNERGISTIC EFFECT FOR THE TiO_2–Fe_2O_3 AND ZrO_2–Fe_2O_3 CATALYSTS

From the above results and discussion, we found that the metal oxides TiO_2, Fe_2O_3 and ZrO_2 showed some kind of synergistic effect for the dehydrogenation of ethylbenzene. By themselves, TiO_2, Fe_2O_3, and ZrO_2 gave 20.3%, 28.5%, and 40.3% conversion and 86%, 79%, and 87% selectivity, respectively. However, the mixed metal oxides TiO_2–Fe_2O_3 (3/1) and ZrO_2–Fe_2O_3 (4/1) gave 44.5 and 44.1% conversion and 80 and 74% selectivity, respectively. The synergistic effect could also be found in the TiO_2–Fe_2O_3–ZrO_2 system. Fig. 8 shows the conversion of ethylbenzene against time on stream for the catalysts TiO_2, Fe_2O_3, ZrO_2, TiO_2–Fe_2O_3, ZrO_2–Fe_2O_3, and TiO_2–Fe_2O_3–ZrO_2, where the commercial catalyst Shell 105 was also compared. The activities of these catalysts can be ranked in the following order: TiO_2–Fe_2O_3–ZrO_2(1/1/1) > TiO_2–Fe_2O_3(3/1) > ZrO_2–Fe_2O_3(4/1) > ZrO_2 > Shell 105 > Fe_2O_3 > TiO_2. Commercial potassium-promoted iron catalyst was considered to be a typical base catalyst. The reaction of ethylbenzene dehydrogenation over this kind of catalyst was known to go through a basic mechanism instead of the acid–base bifunctional mechanism as proposed in our previous papers [4–7].

4. Conclusion

The catalytic activities of TiO_2–Fe_2O_3 and ZrO_2–Fe_2O_3 catalysts for ethylbenzene dehydrogenation were investigated and found to be correlated well with their properties such as acidity, basicity, surface area, and crystallinity. A synergistic effect was found for these catalyst systems. It was concluded that the catalyst TiO_2–Fe_2O_3–ZrO_2 with 1/1/1 molar ratio, TiO_2–Fe_2O_3 with 75 mol% of TiO_2 and ZrO_2–Fe_2O_3 with 80 mol% of ZrO_2 gave the highest activities. Meanwhile, all of

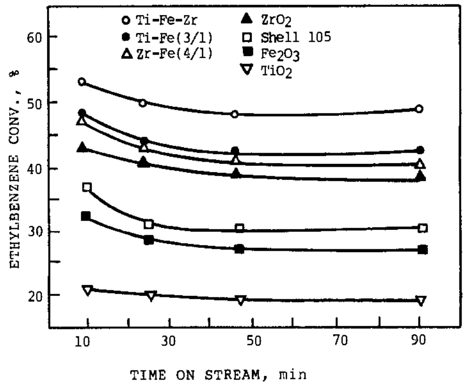

Fig. 8. Comparison of catalytic activities of pure metal oxides TiO_2, ZrO_2 and Fe_2O_3, and mixed metal oxides, TiO_2–Fe_2O_3, ZrO_2–Fe_3O_3 and TiO_2–Fe_2O_3–ZrO_2; reaction temperature, 570°C; WHSV = 11.3.

these catalysts showed higher activities and styrene yields than the conventional K_2O-promoted iron catalysts.

Acknowledgement

The authors with to express their gratitude for the support of this work by the Chemistry Department of Tunghai University and the Refining and Manufacturing Research Center of Chinese Petroleum Corporation.

References

[1] H.W. Scheeline, SRI Report 33B (1977) 73;
Y.C. Yen and T.H. Vanden Bosch, SRI Report 33A (1973) 35;
Y.C. Yen, SRI Report 33 (1967) 91.
[2] B. Delmon, P.A. Jacobs and G. Poncelet, eds., *Preparation of Catalysts II* (Elsevier, Amsterdam, 1979) p. 293.
[3] E.H. Lee, Catal. Rev. 8 (1973) 285.
[4] I. Wang, W.F. Chang, R.J. Shiau, J.C. Wu and C.S. Chung, J. Catal. 83 (1983) 428.
[5] J.C. Wu, C.S. Chung, C.L. Ay and I. Wang, J. Catal. 87 (1984) 98.
[6] I. Wang, J.C. Wu and C.S. Chung, Appl. Catal. 16 (1985) 89.
[7] J.C. Wu, C.S. Chung and I. Wang, Appl. Catal. 18 (1985) 295.
[8] R. Fiedorow, W. Przystazko and M. Sopa, J. Catal. 68 (1981) 33.
[9] Y. Murakami, K. Iwayama, H. Uchida, T. Hattori and T. Tagawa, J. Catal. 71 (1981) 257.
[10] Y. Murakami, K. Iwayama, H. Uchida, T. Hattori and T. Tagawa, Appl. Catal. 2 (1982) 67.
[11] M. Ai, J. Catal. 50 (1977) 291.
[12] M. Ai, J. Catal. 52 (1978) 16.
[13] M. Ai, J. Catal. 60 (1979) 306.
[14] T. Tagawa, T. Hattori and Y. Murakami, J. Catal. 75 (1982) 56.
[15] T. Tagawa, T. Hattori and Y. Murakami, J. Catal. 75 (1982) 66.
[16] S. Matsuda and A. Kato, Appl. Catal. 8 (1983) 149.
[17] H. Hattori, M. Itoh and K. Tanabe, J. Catal. 41 (1976) 46.
[18] Y. Nakano, H. Hattori and K. Tanabe, J. Catal. 57 (1979) 1.
[19] M. Itoh, H. Hattori and K. Tanabe, J. Catal. 35 (1974) 35.
[20] M. Niwa, M. Sago, H. Ando and Y. Murakami, J. Catal. 69 (1981) 69.
[21] H. Hattori, M. Itoh and K. Tanabe, J. Catal. 38 (1975) 172.
[22] K. Tanabe, H. Hattori, T. Sumiyoshi, K. Tamaru and T. Kondo, J. Catal. 53 (1978) 1.
[23] M. Ai, Bull. Chem. Soc. Japan 49 (1976) 1328.
[24] E. Rodenas, T. Yamaguchi, H. Hattori and K. Tanabe, J. Catal. 69 (1981) 434.
[25] K. Tanabe and C. Ishiya, Bull. Chem. Soc. Japan 45 (1972) 47.
[26] M. Itoh, H. Hattori and K. Tanabe, J. Catal. 43 (1976) 192.
[27] A.M. Rubinstein, A.A. Dulov and A.A. Slinkin, J. Catal. 35 (1974) 80.
[28] A. Arata, S. Akutagawa and K. Tanabe, Bull. Chem. Soc. Japan 49 (1976) 390.